Inorganica Chimica Acta, 172 (1990) 233–239

Solid State Dehydration Condensation of Potassium Tetrakis(μ-pyrophosphito-*P,P'*)diplatinate(II) Accompanied by the Red Shift of the Luminescence Peak

TADASHI YAMAGUCHI, YOICHI SASAKI*, TAKESHI IKEYAMA**, TOHRU AZUMI and TASUKU ITO*

Department of Chemistry, Faculty of Science, Tohoku University, Aramaki, Aoba-ku, Sendai 980 (Japan)

(Received September 13, 1989; revised January 4, 1990)

Abstract

Yellow crystals of $K_4[Pt_2(pop)_4]\cdot 2H_2O$ (pop^{2-} = pyrophosphite(2–)) change their color to orange upon dehydration *in vacuo* or at elevated temperatures with concomitant change in the emission color from green (emission peak at 515 nm) to orange (emission peaks at 520, 570, 670 nm). Thermogravimetric, ^{31}P CP-MAS NMR, electronic and infrared absorption spectral studies indicate that the dehydration is not a simple loss of crystalline waters but involves dehydration condensation between the neighboring complex anions. The original green emission is recovered on dissolving the orange solid in water. Emissions from the dehydrated orange solid are of phosphorescence type ($\tau_{em} \leqq 6$ μs). Relative intensity of the three emission peaks depends significantly on dehydration conditions, exciting wavelength and temperature. The orange solid seems to contain various species with different extent and type of condensation. Red shift of the emission peak on dehydration was discussed on the basis of the ligand field theory.

Introduction

Since the discovery of its strong green emission both in the solid state and in aqueous solution [1–3], tetrakis(μ-pyrophosphito-*P,P'*)diplatinate(II) ion, $[Pt_2(pop)_4]^{4-}$, has been extensively studied [4]. The potassium salt is the one that has been most frequently used. The pure potassium salt appears to be yellow [5], but greenish [2, 6, 7], brown [8] and purple [6, 8] salts have also been reported. The latter ones were claimed to show similar luminescence behavior in aqueous solution and considered to be composed of essentially the same compounds as the yellow solid despite the apparent color difference. Gray and coworkers indicated that the greenish salt is contaminated with a small amount of oxidized species, and described a standard method for the preparation of the pure yellow salt [9].

During the course of the study on the photoquenching reactions of the dimeric ion, $[Pt_2(pop)_4]^{4-}$ [10], we observed that yellow crystals of the potassium salt turned orange with concomitant change in emission color to orange. The color changes were observed when the crystals were kept *in vacuo* for several days or dried at elevated temperatures. When the orange solid was dissolved in water, the original green emission was recovered. Such changes were not observed for the contaminated dark green crystals. Since the observed phenomena in the solid state have not been described previously as far as we know, we decided to study further these interesting phenomena. A preliminary account of this work has already been published [11].

Experimental

Preparation of the Complex

Potassium tetrakis(μ-pyrophosphito-P,P')-diplatinate(II) dihydrate, $K_4[Pt_2(pop)_4]\cdot 2H_2O$

This salt was prepared by a method essentially the same as that of Sadler *et al.* [6]. Subtle difference in reaction conditions and recrystallization procedures gave variously colored crystals from yellow to dark green. $K_2[PtCl_4]$ (2 g; 0.0048 mol) and H_3PO_3 (7 g; 0.085 mol) in 10 cm^3 of water was boiled until the solution became pale yellow (7–8 h). The resulting solution was evaporated at 120–130 °C. The yellow residue was washed with methanol and acetone, and recrystallized by either evaporating the aqueous solution at room temperature or keeping the aqueous solution in a refrigerator. According to Gray and coworkers [9], the pure yellow salt is prepared under oxygen free atmosphere. Absence of Cl^- ions is also reported to be preferable for obtaining the pure salt.

*Authors to whom correspondence should be addressed.

**Permanent address: Department of Chemistry, Miyagi University of Education, Aramaki, Aoba-ku, Sendai 980, Japan.

0020-1693/90/$3.50

In this study, we did not try to follow their method, since the yellow crystals were fortunately obtained by the preparation under less strict conditions.

Ammonium salt, $(NH_4)_4[Pt_2(pop)_4]$

The ammonium salt was prepared by the use of $(NH_4)_2[PtCl_4]$ as a starting material instead of $K_2[PtCl_4]$ and by following the method described above. The product was recrystallized from water.

Tetraethylammonium salt, $[(C_2H_5)_4N]_4[Pt_2(pop)_4]$ and lithium salt, $Li_4[Pt_2(pop)_4]$

These salts were prepared by the cation exchange method. An aqueous solution of the potassium salt was passed twice through a cation exchange column of Dowex 50W-X8 in either the $(C_2H_5)_4N^+$ or the Li^+ form. The solution was evaporated to obtain the corresponding salt.

Measurements

Ultraviolet and visible absorption spectra were measured by using a Hitachi 330 spectrophotometer. An integrating sphere attachment was used for the measurement of the reflectance spectra in MgO. Infrared absorption spectra were recorded on a JASCO IR-810 spectrophotometer as KBr pellets at room temperature. X-ray photoelectron spectra were obtained by a VG-ESCA LAB Mark II using Mg Kα excitation radiation at ambient temperature at pressure less than 10^{-9} Torr. Samples were prepared as BN pellets. The energy scale was calibrated by emission from the K $2p_{3/2}$ line at 292.9 eV or the C 1s (methyl carbon) line at 284.6 eV as internal standard. The ^{31}P and ^{195}Pt CP-MAS NMR spectra were measured at JEOL by using a JNM-GSX-270 NMR spectrometer with an attachment for multinuclear solid state high-resolution measurement. The thermogravimetric analyses were carried out by using a Rigaku differential thermogravimetric analyser TG-DSC-8085E1. Emission spectra were obtained with a SPEX Fluorolog 2 emission spectrophotometer, and also with a SPEX 1702 spectrophotometer and a photomultiplier R-928 of Hamamatsu Photonics on irradiation with a nitrogen laser Molectron UV-400. Emission lifetimes were measured by irradiating at 337 nm with an N_2 laser JL-1000L of NDC. The emission decay was followed by a Jovin-Yvon H20V spectrophotometer and a photomultiplier R-955 of Hamamatsu Photonics. The signals were analyzed by using a TS-8121 stragescope of Iwasaki Electric Co. and a microcomputer HP-86 of Hewlett Packard.

Results

We obtained variously colored crystals of $K_4[Pt_2(pop)_4]\cdot 2H_2O$ from yellow to dark green. Only yellow crystals showed the change in color to orange. The color change occurred either by keeping the crystals *in vacuo* at room temperature or by evacuating the crystals at *c.* 120 °C, and was accompanied by many cracks on the surface of the crystals. With respect to the greenish crystals, one lot of green crystals was chosen for detailed studies which showed 'typical' thermogravimetric behavior of the green solid (*vide infra*). Some other greenish crystals showed intermediate thermogravimetric behavior between the yellow and the chosen green crystals. The following experiments were carried out in order to find (i) the cause of the different behaviors of the yellow and the green crystals, and more importantly (ii) the structure and the electronic state of the orange species.

Thermogravimetrical Analysis

Figure 1 shows TG curves for the two kinds of crystals. The yellow crystals started to lose their lattice waters at *c.* 50 °C, the mass loss being *c.* 4.3% at 100 °C. Since the two lattice water molecules correspond to 3.1% of the total mass, it is concluded that dehydration condensation between two coordinated pyrophosphite ligands takes place either within a complex ion or between neighboring ions. The mass loss of *c.* 4.3% corresponds to the loss of one additional water molecule per complex ion. The DSC curve (Fig. 1) clearly shows two endothermic peaks during the mass loss. The green crystals started to lose their lattice waters at a much higher temperature. The 'condensation' seems to occur at >150 °C, since the mass loss was *c.* 2.5% at 150 °C.

X-ray Crystal Structures

Two crystals representing yellow and green ones were chosen. The thermogravimetric behaviors were studied for the same crystals just after the structural determinations in order to confirm the nature of the crystals. The X-ray structural study was not possible for the orange species due to the formation of cracks during the color change. Both yellow and green

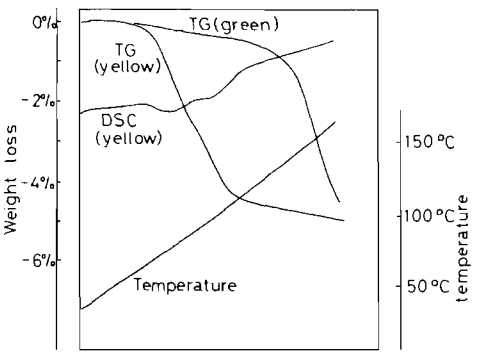

Fig. 1. Thermogravimetric analysis curves of the yellow and the green crystals of $K_4[Pt_2(pop)_4]\cdot 2H_2O$ (see text).

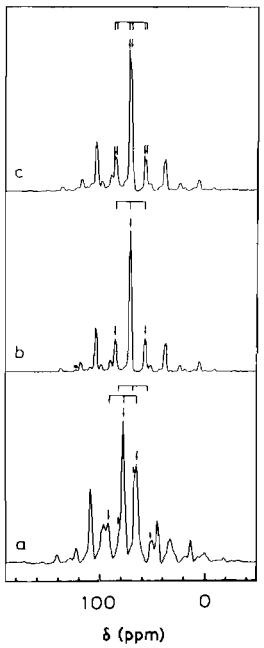

Fig. 2. ^{31}P CP-MAS NMR spectra of (a) the dehydrated orange solid, (b) the yellow, (c) the green crystals of $K_4[Pt_2(pop)_4]\cdot 2H_2O$ as measured at a spinning rate of *c.* 3500 s^{-1}. Arrows indicate signals of the sample.

crystals showed very similar crystal and molecular structures which are also similar to those reported previously [5b, 6]. Meaningful differences were not found between the two crystals, see 'Supplementary Material'.

^{31}P CP-MAS NMR

Solid state ^{31}P NMR spectra (Fig. 2) were measured for the yellow and the green crystals as well as the orange solid. The signals from the samples were assigned by comparing the spectra at different spinning rates. The yellow crystals showed one sharp signal at 71.7 ppm (versus 85% H_3PO_4 in D_2O at $\delta = 0$) with $J(Pt-P) = 3105$ Hz. The corresponding signal of the green crystals splitted into two peaks at 70.6 and 72.0 ppm with similar intensity. The $J(Pt-P)$ was 3095 Hz. The orange solid showed a significantly different spectral pattern. Two groups of ^{31}P NMR signals appeared at *c.* 66 and 77.2 ppm. The former signal was much smaller in intensity*. The ^{31}P nuclei of $[Pt_2(pop)_4]^{4-}$ in aqueous solution were reported to resonate at 66.5 [12], 69.4 ($J(Pt-P) = 3248$ [5] or 3095 Hz [13]) or 66.14 (3073 Hz) [9] ppm.

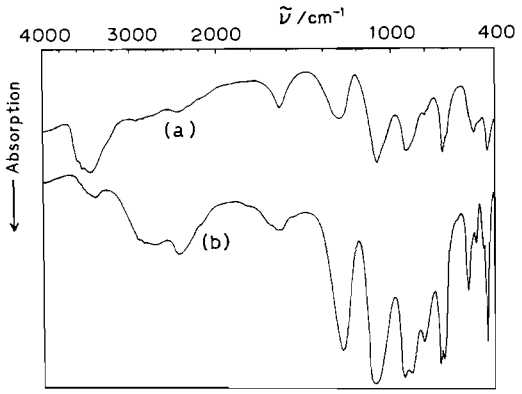

Fig. 3. Infrared absorption spectra of (a) the yellow crystals and (b) the dehydrated orange solid.

Electronic Absorption Spectra

Both yellow and green crystals showed the typical absorption spectral pattern of $[Pt_2(pop)_4]^{4-}$ in aqueous solution with an intense peak at 368 nm and a weak one at 450 nm [2, 3]. The diffuse reflectance spectrum in KBr pellet of the green crystals showed a broad peak around 600 nm, which was absent in the yellow crystals. A small amount of oxidized species in the green crystals [9] may be responsible for the observed band at around 600 nm**.

The dehydrated orange solid in KBr pellet shows two broad absorption maxima centered at *c.* 400 and 470 nm.

Infrared Absorption Spectra

Spectra of the yellow and the green crystals did not show an appreciable difference from one another and coincided with the reported ones [15]. That of the orange solid was, however, clearly different in some points from those of the two crystalline species (Fig. 3). Some peaks related to ligand vibrations [15], such as PO_2 bending at 400–500 cm^{-1}, P–O(P) stretching at 700 cm^{-1} and $PO_{(terminal)}$ stretching at 920 cm^{-1}, showed splitting patterns in the orange solid. Furthermore, a new peak was observed at 800 cm^{-1} and the POH bending peak clearly appeared at a lower energy region (1280 cm^{-1}) than that of the yellow crystals (1320 cm^{-1}).

Emission Spectra

The solid state emission spectrum of the yellow crystals showed a strong phosphorescence peak at

*^{195}Pt CP-MAS NMR of the three solids were also measured. The spectra were not well resolved and less informative. All the solids gave signals centered at around −5000 ppm. The signal of the dimer ion in aqueous solution was reported to appear at −5123 [6] or −5139 [13] ppm.

**$K_4[Pt_2(pop)_4Cl]$ in KCl pellet was reported to show a broad absorption band at around 600 nm [5b], while the compound in nujol mull showed a band at 512 nm [14]. $[Pt_2(pop)_4Cl_2]^{4-}$ does not show any strong absorption band in visible region [9, 14].

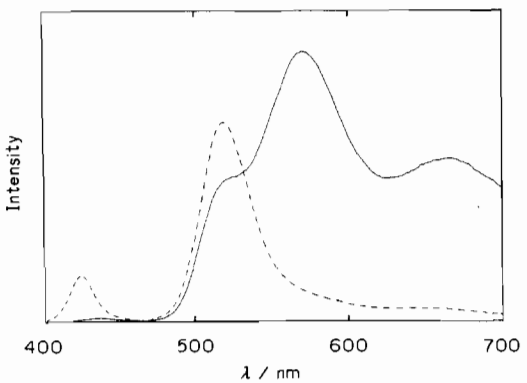

Fig. 4. Solid state emission spectra of one of the dehydrated solids (——) and the original yellow crystals of $K_4[Pt_2(pop)_4]\cdot 2H_2O$ (- - - -) on irradiation at 368 nm.

518 nm and a weak fluorescence peak at 424 nm* (Fig. 4) at room temperature on irradiation at 368 nm**. In aqueous solution, the relative intensity of the phosphorescence peak (515 nm) was much stronger to the fluorescence.

Figure 4 also shows a typical example of the emission spectra of the dehydrated orange solid. There were three emission peaks at *c.* 520, 570 and 670 nm. The relative intensity of the three peaks differed appreciably among samples prepared under various dehydration conditions. The emission peak at the highest energy region appeared at slightly lower energy than the phosphorescence of the yellow crystals. The relative intensity of the three new emissions also depended on the change in the excitation wavelength in the range from 370 to 470 nm. Excitation at longer wavelengths caused an increase in relative intensity of the emissions at longer wavelengths. Excitation spectra for the 520 and 570 nm emissions showed a weak peak at 430 nm and a broad one at 460 nm, respectively. The 670 nm emission showed a broad peak beyond 500 nm in its excitation spectrum. The emission spectrum also showed significant temperature dependence. At lower temperatures, relative intensity of the emission peak at the highest energy increased remarkably.

A careful measurement of the emission at 4.2 K demonstrated vibrational structures for the peak at *c.* 520 nm. The excitation wavelength was 337.1 nm. Two sets of the progression both in a 115 cm^{-1} vibration were observed. The initial yellow species was reported to show the 118 [2] or 115 [5a] cm^{-1} progression which corresponds to the ground state Pt–Pt stretching vibration [14–16].

When the dehydration was continued at 200 °C, the new emission peak appeared at *c.* 730 nm in addition to the three emission peaks.

Emission Lifetimes

Emission decays were followed at three emission regions of the orange species at room temperature. The emission decays did not show exponential behavior. From the initial part of the decay, the lifetimes, τ_{em}, were roughly estimated to be *c.* 2 and 6 μs for the emission peaks at 570 and 670 nm, respectively. The lifetime of the emission at 520 nm was much shorter (<0.3 μs). The phosphorescence lifetime of the yellow crystals is 5.5 μs at 300 K [17]. Emissions of the orange solid are of the phosphorescence type. The result clearly shows that the 520 nm emission of the orange salt does not arise from the uncondensed dimer, if any.

X-ray Photoelectron Spectra

The Pt $4f_{7/2}$ and P 2p binding energies of the dehydrated orange potassium salt were 73.2 and 133.1 eV, respectively. The yellow crystals can undergo dehydration under high vacuum circumstances of the XPS chamber. The tetraethylammonium salt which is not expected to undergo dehydration condensation (*vide infra*), showed similar binding energies, i.e. 73.2 and 133.3 eV for Pt $4f_{7/2}$ and P 2p, respectively. These results clearly show that the platinum atoms of the dimer in the potassium salt remain divalent after the dehydration condensation. The binding energies for the dehydrated potassium salt are in reasonable agreement with those reported previously for $K_4[Pt_2(pop)_4]$ (73.3 and 133.2 eV) [9, 18] which could be in the dehydrated state†.

Experiments with Other Salts

The dehydration behaviors of the ammonium and the tetraethylammonium salts were briefly investigated. The green crystals of the ammonium salt changed their color partly to orange upon dehydration at elevated temperatures. The dehydrated solid showed a small emission peak at *c.* 600 nm in addition to the strong peak at 522 nm. The tetraethylammonium salt did not change color even at *c.* 180 °C.

*The phosphorescence peak appeared at somewhat longer wave length than that in aqueous solution (*c.* 407 nm) [2, 3].

**The green salts showed much weaker emission: phosphorescence at 513 nm and fluorescence at 420 nm with a similar intensity. The difference from the yellow crystals may be explained by considering extensive quenching of the phosphorescence in the green crystals. Quenching may be related to the existence of the oxidized species as an impurity (the oxidized species may act as a quencher). In aqueous solution, the emission spectrum is similar to that of the yellow crystals in water.

†Binding energies in refs. 9 and 18 were corrected for our standard (aliphatic carbon at 284.6 eV and potassium ion at 292.9 eV as internal standard).

Discussion

Differences between the Yellow and the Green Crystals

A distinctive difference between the two crystals was observed in their thermogravimetric behaviors. An ORTEP drawing of the crystal structure of the yellow one is shown in Fig. 5. The green crystal has an almost identical crystal structure. The difference between the crystal structures of the yellow and the green crystals is too small to account for the different thermogravimetric behaviors of the yellow and the green crystals.

Solid state ^{31}P NMR spectroscopy of the green crystals showed that there are two types of nearly equal amounts of phosphorus atoms at different chemical environments. Since the impurity (oxidized dimer) in the green crystals is only a small amount, neither of the two ^{31}P NMR peaks can be assigned to it. Under the adopted symmetry of the crystal, all the phosphorus atoms are equivalent and a water oxygen atom is situated at equal distances from the four neighboring PO_2 moieties. If we consider the hydrogen atoms of the water molecule at directions of two particular PO_2 moieties, then the four PO_2 groups are discriminated. Although the Ow–O1 (see Fig. 5) distance (3.35 Å) is a bit too long for a hydrogen bond, the splitting of the ^{31}P NMR signal of the green crystals can only be explained by assuming some interactions between a hydrogen and oxygens. The interaction is not important in the yellow crystals as indicated by the single ^{31}P NMR peak, and the crystalline water molecules may be released more easily.

The thermogravimetric and ^{31}P NMR spectral studies indicated that a small amount of the oxidized dimer must affect the whole crystal system. From the available data alone, it is not possible to explain convincingly why all the crystalline waters in the green crystals are more difficult to remove than those in the yellow crystals.

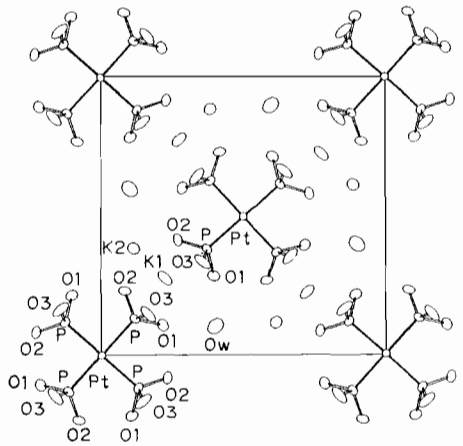

Fig. 5. An ORTEP drawing of the crystal structure of the yellow crystal of $K_4[Pt_2(pop)_4]\cdot 2H_2O$ together with atomic numbering scheme.

Nature of the Orange Species

From the mass loss of the dehydration of the yellow crystals to give the orange species, dehydration condensation between the ligands should take place (one water molecule per complex ion). Since the characteristic green emission of the original yellow species is recovered when the orange solid is dissolved in water, the dehydration process should be simple and not involve any irreversible breakage of the basic structural unit. Intramolecular dehydration appears to be difficult to achieve since it must be accompanied by considerable distortion within the complex ion. Intermolecular dehydration can take place either in the direction of the Pt–Pt axis of the complex ion, or perpendicular to the Pt–Pt axis (see Fig. 5). Both methods of condensation appear to be possible.

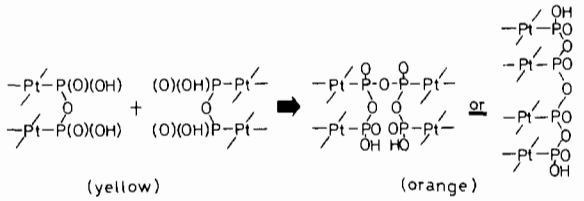

Scheme 1.

The condensation may give a tetramer by double condensations of two dimers. Alternatively condensation polymerization may take place. Easy loss of the crystalline waters of the yellow crystals makes the approach of the two complex anions easier and leads to dehydration condensation.

The ^{31}P CP-MAS NMR of the dehydrated solid showed two peaks at 77.2 and *c.* 66 ppm with the latter having a much smaller intensity. One fourth of the phosphorus atoms should be involved in the intermolecular P–O–P bond, since condensation occurs once per one complex anion on the basis of the weight loss. The NMR peak at *c.* 66 ppm should then be assigned to the phosphorus atoms involved in the new P–O–P bridge. Splitting of the infrared bands related to the PO part is consistent with the proposed dehydration condensation.

The dependence of emission spectra on various factors and the different lifetime of each emission peak, indicate that the three emission peaks are independent from one another and should arise from different emission centers. The orange species may be composed of various species with different extents of condensation.

Observation of the vibrational structures (progression of 115 cm^{-1}) at low temperatures indicates that the nature of the emission (at 520 nm at least) is

basically the same as that of the original dimer [2, 3, 5a]. Since the progression is very similar to that of the original species [14–16], the Pt–Pt distance does not change significantly on dehydration condensation.

Origin of the Red Shift of the Emission

The red shift of the $\sigma^*(5d_{z^2})$ to $\sigma(6p_z)$ transition band of the dimeric species upon an increase of the metallic chain length by condensation, has been noted for some platinum(II) and rhodium(I) species [19, 20]. The oligomeric form of the present dimeric species has also been reported, which is bluish in color and considered to contain an oligomeric condensed phosphite chain with more than three linearly arranged platinum(II) ions [21]. This species shows intense red emission centered at 650 nm. A Raman signal at 85 cm^{-1} of ν(Pt–Pt) coincides with the calculation for the linear triplatinum model [21]. In the present case, the Pt–Pt dimeric unit seems to be preserved as far as the emission at *c.* 520 nm (progression at 115 cm^{-1}) of the orange solid is concerned. For the species responsible for the longer wavelength emission, it is not clear if the metal–metal interaction extends to the neighboring dimeric unit. However, reversibility of condensation seems to indicate that even in these species Pt–Pt interaction is likely to be preserved within the dimeric unit and inter-unit interaction, if present, should not be significant.

Under the assumption that the dimeric unit is basically preserved, the state energy is determined by three factors, i.e. the strength of the ligand field, the metal–metal interaction and the spin orbit coupling. Among them, the change in the ligand field is the most probable cause of the observed red shift in the phosphorescence. The metal–metal interaction and the spin–orbit coupling are expected to be independent of the ligand field strength. Therefore, the transition energy of the dimeric complex preserves the change in energies of the corresponding atomic orbitals of each platinum in the given ligand field.

Basicity of the coordinated phosphorous atom would increase by dehydration because the hydrogen bond is removed. Accordingly, the ligand field is likely to increase as a result of dehydration.

For the purpose of clarifying an effect of dehydration on the transition energy of the phosphorescence, the simple ligand field theory [22] is applied to estimate the change in energy of the atomic orbitals of a platinum atom under the assumption that only the strength of the ligand field varies by dehydration. In this model, the complex contains four indentical ligands (charged $-Ze$ and located at a distance a from the metal center) arranged in a square (in xy-plane, Pt–Pt direction is taken as z-axis), and one electron is located at the metal center. The potential of the tetragonal (D_{4h}) ligand field can be expanded in a series of spherical harmonics as follows

$$V_{\text{tetra}}(r,\theta,\phi) = 4Ze^2/a - (2Ze^2/a^3)r^2C_0^{(2)}(\theta,\phi) + (3Ze^2/2a^5)r^4[C_0^{(4)}(\theta,\phi) + \sqrt{35}/3\sqrt{2}(C_4^{(4)}(\theta,\phi) + C_4^{(4)}(\theta,\phi)] + (\text{higher order terms}) \quad (1)$$

where $C_m^{(k)}(\theta,\phi) = (4\pi/(2k+1))^{1/2}Y_{km}(\theta,\phi)$. As far as p and d orbitals are concerned, the matrix element of the higher energy terms in the above Hamiltonian vanishes. The energies of orbitals which are responsible for the transition of our interest are

$$E(5d_{z^2}) - E^0(5d) = 4Ze^2/a - (4/7)(Ze^2/a^3)\langle R_{52}|r^2|R_{52}\rangle + (3/7)(Ze^2/a^5)\langle R_{52}|r^4|R_{52}\rangle \quad (2)$$

$$E(6p_z) - E^0(6p) = 4Ze^2/a - (4/5)(Ze^2/a^3)\langle R_{61}|r^2|R_{61}\rangle \quad (3)$$

where $E^0(5d)$ and $E^0(6p)$ are the corresponding orbital energies of the spherical atom, and $\langle R_{nl}|r^k|R_{nl}\rangle = \int_0^\infty R_{nl}r^kR_{nl}r^2\,dr$. The ratios

$$\langle R_{52}|r^4|R_{52}\rangle/a^2\langle R_{52}|r^2|R_{52}\rangle = 0.66 \quad (4)$$

$$\langle R_{61}|r^2|R_{61}\rangle/\langle R_{52}|r^2|R_{52}\rangle = 3.1 \quad (5)$$

are obtained by using Slater orbitals $|R_{nl}\rangle$ (in which orbital exponents are determined by the Slater recipe) and using $a = 2.315$ Å (Pt–P distance of the yellow crystal).

By using these results the orbital energies $E(5d_{z^2})$ and $E(6p_z)$ are calculated as a function of the parameter $(Ze^2/a^3)\langle R_{52}|r^2|R_{52}\rangle$ which represents the strength of the ligand field. The result is shown in Fig. 6, in which energies of the other orbitals ($5d_{x^2-y^2}$, $5d_{xy}$, etc.) are also shown. Figure 6 shows that as the ligand field strength increases the $5d_{z^2}$ orbital energy increases more significantly than that of the $6p_z$. Thus the transition energy decreases as the ligand field increases. These calculations qualitatively explain the red shift observed here.

Supplementary Material

Experimental details on the crystal structure determination, tables of crystal data and data collection parameters, of the atomic positional parameters and the thermal parameters, and of the structure factors are available on request from the authors.

Acknowledgements

We are grateful to Drs K. Toriumi (Institute for Molecular Science, Okazaki) and M. Ebihara (Gifu

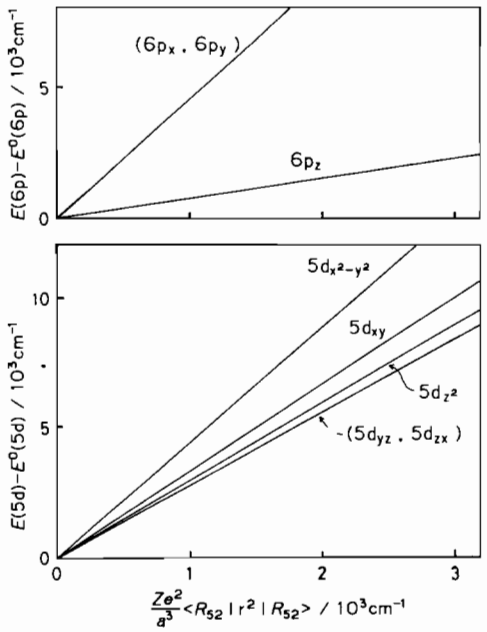

Fig. 6. Energies of 5d and 6p atomic orbitals as a function of the parameter $(Ze^2/a^3)\langle R_{52}|r^2|R_{52}\rangle$ which represents the strength of the ligand field (see text).

University) for the X-ray crystal structure analysis. CP-MAS NMR spectra were measured at JEOL to which authors thanks are due. This work was partly supported by Grant-in-Aid for Scientific Research (No. 01430009) on Priority Area of 'Dynamic Interactions and Electronic Processes of Macromolecular Complexes' from the Ministry of Education, Science and Culture, Japan.

References

1 R. P. Sperline, M. K. Dickson and D. M. Roundhill, *J. Chem. Soc., Chem. Commun.*, (1977) 62.
2 W. A. Fordyce, J. G. Brummer and G. A. Crosby, *J. Am. Chem. Soc., 103* (1981) 7061.
3 C.-M. Che, J. G. Butler and H. B. Gray, *J. Am. Chem. Soc., 103* (1981) 7796.
4 (a) M. Fetterolf, A. E. Friedman, Y.-Y. Yang, H. Offen and P. C. Ford, *J. Phys. Chem., 92* (1988) 3760; (b) J. K. Nagle and B. A. Brennan, *J. Am. Chem. Soc., 110* (1988) 5931; (c) C.-M. Che, H.-L. Kwong and K.-C. Cho, *Inorg. Chem., 27* (1988) 3691; (d) C.-M. Che, W.-H. Lee and K.-C. Cho, *J. Am. Chem. Soc., 110* (1988) 5407; (e) D. M. Roundhill, Z.-P. Shen, C. King and S. J. Atherton, *J. Phys. Chem., 92* (1988) 4088; (f) C.-M. Che, W.-H. Lee, K.-C. Cho, P. D. Harvey and H. B. Gray, *J. Phys. Chem., 93* (1989) 3095; (g) C. King, Y. Yin, G. L. McPherson and D. M. Roundhill, *J. Phys. Chem., 93* (1989) 3451; (h) D. M. Roundhill, H. B. Gray and C.-M. Che, *Acc. Chem. Res., 22* (1989) 55, and refs. therein.
5 (a) S. F. Rice and H. B. Gray, *J. Am. Chem. Soc., 105* (1983) 4571; (b) C.-M. Che, F. H. Herbstein, W. P. Schaefer, R. E. Marsh and H. B. Gray, *J. Am. Chem. Soc., 105* (1983) 4604.
6 F. A. Filomena Ros Remedios Pinto, P. J. Sadler, S. Neidle, M. R. Sanderson, A. Subbiah and R. Kuroda, *J. Chem. Soc., Chem. Commun.*, (1980) 13.
7 M. K. Dickson, S. K. Pettee and D. M. Roundhill, *Anal. Chem., 53* (1981) 2159.
8 J. T. Markett, D. P. Clements, M. R. Corson and J. K. Nagle, *Chem. Phys. Lett., 97* (1983) 175.
9 C.-M. Che, L. G. Butler, P. J. Grunthaner and H. B. Gray, *Inorg. Chem., 24* (1985) 4662.
10 T. Yamaguchi and Y. Sasaki, *Inorg. Chem., 29* (1990) 423.
11 T. Yamaguchi, Y. Sasaki, T. Ikeyama, T. Azumi and T. Ito, *J. Coord. Chem., 18* (1988) 223.
12 S. A. Bryan, M. K. Dickson and D. M. Roundhill, *Inorg. Chem., 26* (1987) 3878.
13 C. King, D. M. Roundhill, M. K. Dickson and F. R. Fronczek, *J. Chem. Soc., Dalton Trans.*, (1987) 2769.
14 M. Kurmuoo and R. J. H. Clark, *Inorg. Chem., 24* (1985) 4420.
15 P. Stein, M. K. Dickson and D. M. Roundhill, *J. Am. Chem. Soc., 105* (1983) 3489.
16 C.-M. Che, L. G. Butler, H. B. Gray, R. M. Crooks and W. H. Woodruff, *J. Am. Chem. Soc., 105* (1983) 5492.
17 Y. Shimizu, Y. Tanaka and T. Azumi, *J. Phys. Chem., 88* (1984) 2423.
18 L. G. Butler, W. H. Zietlow, C.-M. Che, W. P. Schaefer, S. Sridar, P. J. Grunthaner, B. I. Swanson, R. J. Clark and H. B. Gray, *J. Am. Chem. Soc., 110* (1988) 1155.
19 T. Kawamura, T. Ogawa, T. Yamabe, H. Masuda and T. Taga, *Inorg. Chem., 26* (1987) 3547.
20 I. S. Sigal and H. B. Gray, *J. Am. Chem. Soc., 103* (1981) 2220, and refs. therein.
21 M. K. Dickson, W. A. Fordyce, D. M. Appel, K. Alexander, P. Stein and D. M. Roundhill, *Inorg. Chem., 21* (1982) 3858.
22 S. Sugano, Y. Tanabe and H. Kamimura, *Multiplets of Transition-Metal Ions in Crystals*, Academic Press, New York, 1970, Ch. 1.